

CMS results for the $\gamma\gamma$ production at the LHC: do they give a hint for a Higgs boson of the maximally CP symmetric two-Higgs-doublet model?

M. Maniatis*

Centro de Ciencias Exactas, Universidad del Bío-Bío, Casilla 447, Chillán, Chile

O. Nachtmann†

*Institut für Theoretische Physik, Universität Heidelberg,
Philosophenweg 16, D-69120 Heidelberg, Germany*

Recent measurements of the CMS experiment at the LHC show possibly, with about 3σ significance, a resonance in di-photon events with an invariant mass of 95.4 GeV. If this resonance can be confirmed, this could be a hint for a new elementary particle beyond the Standard Model. An additional Standard-model-like Higgs boson with this mass could be excluded by the CMS experiment. We investigate whether this resonance could fit into a two-Higgs-doublet model highly constrained by CP symmetry, the so-called maximally-CP-symmetric model (MCPM). Our finding shows that indeed the enhancement measured by CMS could originate from the pseudoscalar Higgs boson h'' of this model. According to the model the boson h'' would mainly be produced in the Drell-Yan reaction by charm-anticharm-quark fusion. The main decay mode of h'' is predicted to be $h'' \rightarrow c\bar{c}$. We then consider the so called oblique parameters S , T , U which give us an allowed region for the mass of the scalar Higgs boson h' versus that of the charged ones H^\pm of the MCPM. We calculate the effect of these charged bosons H^\pm in the leptonic decay of the charm-strange mesons D_s^\pm . Our results indicate that the mass m_H of the charged Higgs bosons H^\pm of the MCPM should be around 300 GeV.

I. INTRODUCTION

The search for physics beyond the Standard Model (SM) is a central topic of the current experiments at the LHC. One can, for instance, ask if there exist Higgs bosons in addition to the one Higgs boson of the SM, which by now is well established; see e.g. [1]. One possible extension of the SM is to a model with two Higgs doublets, a 2HDM. There are many such models on the market; see for instance [2–16].

In this work we shall deal with the maximally-CP-symmetric model, the MCPM, as introduced in [17]. A short description of this model is given in [18]. Phenomenological consequences of the MCPM have been presented by us in [19, 20]. As in all 2HDMs the MCPM contains as physical Higgs bosons three neutral ones, denoted by us as ρ' , h' , h'' , and a pair of charged Higgs bosons H^\pm . The boson ρ' of the MCPM behaves very much like the SM Higgs boson. The scalar h' and the pseudoscalar h'' behave quite differently. Their main production mode in proton–proton collisions is the Drell-Yan reaction $c + \bar{c} \rightarrow h', h''$. Important decay modes are $h', h'' \rightarrow c\bar{c}$. But there are also the decays $h', h'' \rightarrow \gamma\gamma$. Therefore, the reaction $p + p \rightarrow \gamma + \gamma + X$ is suitable to search for the neutral Higgs bosons h' and h'' of the MCPM.

Recently the CMS collaboration has published results for $p + p \rightarrow \gamma + \gamma + X$ from the LHC at center-of-mass

energy $\sqrt{s} = 13$ TeV [21]. The search was for a SM-like Higgs boson in the mass range 70 to 110 GeV. A possible enhancement of the $\gamma\gamma$ yield compared to the expectation under the background-only hypothesis has been observed for an invariant $\gamma\gamma$ mass $m_{\gamma\gamma} = 95.4$ GeV; see Figs. 1 and 2.

As we see from Fig. 1 the possible enhancement of the product cross-section for Higgs production σ_H times branching ratio $B(H \rightarrow \gamma\gamma)$ is of order

$$\sigma_H \times B(H \rightarrow \gamma\gamma) \approx 0.01 - 0.04 \text{ pb.} \quad (1)$$

Very interesting are the local p values shown in Fig. 2. The upward fluctuation of $\sigma_H \times B(H \rightarrow \gamma\gamma)$ occurred at the same mass value $m_H = 95.4$ GeV for all CMS runs. In [21] the local (global) significance of the possible effect observed at 95.4 GeV is given as 2.9σ (1.3σ). In [22] a detailed combination of relevant ATLAS, CMS and LEP results was performed and an effect at ≈ 95 GeV with a global significance of 3.8σ was extracted.

We see from Fig. 1 that an additional SM-like Higgs boson at a mass of 80 to 110 GeV is clearly excluded. In the present paper we investigate the question if the possible enhancement of $\gamma\gamma$ production at 95.4 GeV could be due to the production and decay of the boson h'' or h' in the MCPM. Let us also mention the discussion of the 2HDM with an additional complex singlet [23] with respect to the possible resonance at 95.4 GeV. In [24] a model with two Higgs doublets, a real scalar singlet and a Higgs triplet was presented.

Our paper is organised as follows. To make the paper self contained we recall in Sec. II the main features of the MCPM. Sec. III presents our results for an MCPM

* maniatis8@gmail.com

† O.Nachtmann@thphys.uni-heidelberg.de

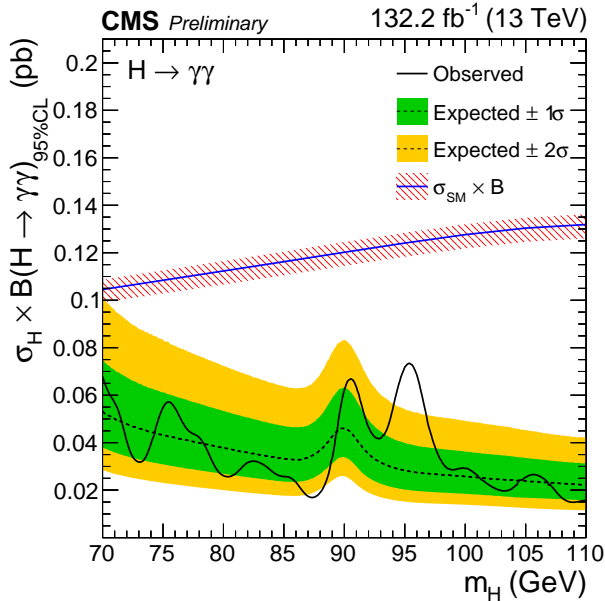


Figure 1. Results for $\sigma_H \times B(H \rightarrow \gamma\gamma)$ from CMS for an additional SM-like Higgs boson; see Fig. 5 of [21]. The green and yellow bands represent the 1σ and 2σ intervals for the background-only hypothesis. The line $\sigma_{\text{SM}} \times B$ with the hatched band represents the expectation for a SM-like Higgs boson in this mass range.

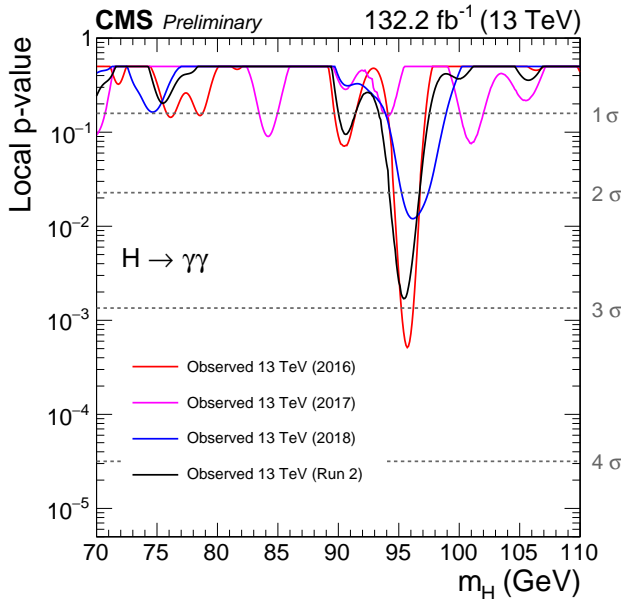


Figure 2. Here we show Fig. 7 of [21] which gives the local p -values for an additional SM-like Higgs boson in the mass range 70-110 GeV. The results for various CMS runs are shown.

Higgs boson of 95.4 GeV mass. In Sec. IV we compare with experiment and discuss our findings. Sec. V deals with leptonic decays of the charm-strange mesons D_s^\pm in view of effects of the charged boson H^\pm of the MCPM in

these decays. Our conclusions are drawn in Sec. VI.

II. BASICS OF THE MCPM

The MCPM has been introduced first in [17] and a short description of it can be found in [18]. For the convenience of the reader we outline here the essential features of the MCPM.

The MCPM is a two-Higgs-doublet model, 2HDM. It has the two Higgs-boson doublets,

$$\varphi_1 = \begin{pmatrix} \varphi_1^+ \\ \varphi_1^0 \end{pmatrix}, \quad \varphi_2 = \begin{pmatrix} \varphi_2^+ \\ \varphi_2^0 \end{pmatrix}. \quad (2)$$

Both are assumed to have weak hypercharge $y = 1/2$. It is convenient to use the K formalism, which works with the gauge-invariant bilinears [25–27],

$$K_0 = \varphi_1^\dagger \varphi_1 + \varphi_2^\dagger \varphi_2 = (\varphi_1^\dagger, \varphi_2^\dagger) \begin{pmatrix} \varphi_1 \\ \varphi_2 \end{pmatrix},$$

$$\mathbf{K} = \begin{pmatrix} K_1 \\ K_2 \\ K_3 \end{pmatrix} = \begin{pmatrix} \varphi_1^\dagger \varphi_2 + \varphi_2^\dagger \varphi_1 \\ i\varphi_2^\dagger \varphi_1 - i\varphi_1^\dagger \varphi_2 \\ \varphi_1^\dagger \varphi_1 - \varphi_2^\dagger \varphi_2 \end{pmatrix} = (\varphi_1^\dagger, \varphi_2^\dagger) \boldsymbol{\sigma} \begin{pmatrix} \varphi_1 \\ \varphi_2 \end{pmatrix}. \quad (3)$$

Here $\boldsymbol{\sigma} = (\sigma^1, \sigma^2, \sigma^3)^T$ and σ^a ($a = 1, 2, 3$) are the Pauli matrices. Basis changes of the Higgs fields (2)

$$\varphi_i(x) \rightarrow \varphi'_i(x) = U_{ij} \varphi_j(x), \quad U = (U_{ij}) \in U(2), \quad (4)$$

correspond to $SO(3)$ rotations in K space

$$K_0(x) \rightarrow K'_0(x) = K_0(x),$$

$$K_a(x) \rightarrow K'_a(x) = R_{ab}(U) K_b(x), \quad (5)$$

where

$$U^\dagger \sigma^a U = R_{ab}(U) \sigma^b, \quad R(U) = (R_{ab}(U)) \in SO(3). \quad (6)$$

In this formalism the most general Higgs potential reads

$$V = \xi_0 K_0 + \boldsymbol{\xi}^T \mathbf{K} + \eta_{00} K_0^2 + 2K_0 \boldsymbol{\eta}^T \mathbf{K} + \mathbf{K}^T E \mathbf{K}. \quad (7)$$

Here the parameters ξ_0 , η_{00} , the 3-component vectors $\boldsymbol{\xi}$, $\boldsymbol{\eta}$, and the symmetric 3×3 matrix $E = E^T$ are all real.

Now we come to generalised CP (GCP) transformations which are generically of the form

$$\varphi_i(x) \rightarrow U_{ij} \varphi_j^*(x'), \quad x = (x^0, \mathbf{x})^T, \quad x' = (x^0, -\mathbf{x})^T,$$

$$U = (U_{ij}) \in U(2). \quad (8)$$

As can be seen from (3) in K space this corresponds to

$$K_0(x) \rightarrow K_0(x'), \quad \mathbf{K}(x) \rightarrow \tilde{R} \mathbf{K}(x'), \quad (9)$$

where \tilde{R} is an improper rotation matrix, $\det(\tilde{R}) = -1$. For a GCP transformation we require that applying it

twice gives back the unit transformation in K space, $\tilde{R}^2 = \mathbb{1}_3$. This leads to two types of GCPs:

- (i) $\tilde{R} = -\mathbb{1}_3$, point reflection in K space,
- (ii) $\tilde{R} = R^T \tilde{R}_2 R$, reflection on a plane in K space,
where $\tilde{R}_2 = \text{diag}(1, -1, 1)$, $R \in SO(3)$.

The standard CP transformation for the Higgs fields has $U_{ij} = \delta_{ij}$ in (8) corresponding to $\tilde{R} = \tilde{R}_2$ in (9), that is, to a reflection on the 1—3 plane in K space.

In [17] the question was studied if one could have a 2HDM allowing the GCP of type (i) as an exact symmetry and how the corresponding symmetric Yukawa term in the Lagrangian would look like. The potential of such a theory, which was called *maximally-CP-symmetric model* (MCPM), must be invariant under $\mathbf{K} \rightarrow -\mathbf{K}$ and, therefore, see (7),

$$V_{\text{MCPM}} = \xi_0 K_0 + \eta_{00} K_0^2 + \mathbf{K}^T E \mathbf{K}. \quad (11)$$

We can choose a basis for the Higgs fields where $E = E^T$ is diagonal,

$$E = \text{diag}(\mu_1, \mu_2, \mu_3), \quad (12)$$

and the eigenvalues are ordered

$$\mu_1 \geq \mu_2 \geq \mu_3. \quad (13)$$

From theorem 5 of [27] we know that the potential (11) leads to a stable theory with the correct electroweak symmetry breaking (EWSB) and no zero mass charged Higgs boson if and only if

$$\begin{aligned} \eta_{00} > 0, \quad \mu_a + \eta_{00} > 0, \quad \text{for } a = 1, 2, 3, \\ \xi_0 < 0, \quad \mu_3 < 0. \end{aligned} \quad (14)$$

The GCP symmetry of type (i) is automatically spontaneously broken by EWSB. In [17] the couplings of the Higgs fields (2) to fermions were studied, requiring invariance under the GCP type (i) symmetry transformation. It turned out that for a single fermion family this symmetry required zero coupling. This finding can be interpreted as giving us a symmetry reason for the existence of more than one fermion family in nature.

For two families the requirement was in essence GCP type (i) symmetry and absence of large flavour-changing neutral currents. This led to the result that one family could have non-zero masses, the other one had to be massless. Adding a third family, uncoupled to the Higgs fields, the MCPM was obtained. For the details of these argumentations we refer to [17].

Before EWSB the Yukawa couplings of the MCPM are highly symmetric. The third family, t , b , τ , couples to the Higgs field φ_1 proportional to the masses m_t , m_b , m_τ , respectively. The second family c , s , μ is in

the strict symmetry limit massless and couples to the Higgs field φ_2 but proportional to the masses of the *third* family, m_t , m_b , m_τ . The first family u , d , e is uncoupled to the Higgs fields and is also massless in the strict symmetry limit.

The Cabibbo-Kobayashi-Maskawa (CKM) Matrix V ,

$$V = \begin{pmatrix} V_{ud} & V_{us} & V_{ub} \\ V_{cd} & V_{cs} & V_{cb} \\ V_{td} & V_{ts} & V_{tb} \end{pmatrix}, \quad (15)$$

is required to be the unit matrix in the strict symmetry limit of the MCPM,

$$V_{\text{MCPM}} = \mathbb{1}_3. \quad (16)$$

Clearly, the strict symmetry limit of the MCPM cannot give an exact representation of what is observed in nature. But, as discussed in [17], the MCPM could be a first approximation to what is observed. Indeed, the masses of the first- and second-family fermions are rather small compared to those of the corresponding third-family masses. Using the central mass values as quoted in PDG [28], which are, except for the top-quark mass $\overline{M_S}$ masses, we get:

$$\begin{aligned} \frac{m_e}{m_\tau} &= 2.88 \times 10^{-4}, & \frac{m_\mu}{m_\tau} &= 5.95 \times 10^{-2}, \\ \frac{m_u}{m_t} &= 1.25 \times 10^{-5}, & \frac{m_c}{m_t} &= 7.35 \times 10^{-3}, \\ \frac{m_d}{m_b} &= 1.12 \times 10^{-3}, & \frac{m_s}{m_b} &= 2.23 \times 10^{-2}. \end{aligned} \quad (17)$$

Also, the CKM matrix V is close to the unit matrix. This is best seen in the Wolfenstein parametrisation [28–31] where

$$V = \begin{pmatrix} 1 - \lambda^2/2 & \lambda & A\lambda^3(\rho - i\eta) \\ -\lambda & 1 - \lambda^2/2 & A\lambda^2 \\ A\lambda^3(1 - \rho - i\eta) & -A\lambda^2 & 1 \end{pmatrix} + \mathcal{O}(\lambda^4) \quad (18)$$

with

$$\lambda \approx 0.23, \quad A \approx 0.83, \quad \rho \approx 0.16, \quad \eta \approx 0.35; \quad (19)$$

see (12.5) and (12.26) in the review 12 of [28].

In [18–20] phenomenological predictions, respectively estimates, for the properties of the physical Higgs bosons of the MCPM were made. Where necessary for phase space reasons fermion masses were introduced by hand. But we think that, nevertheless, this procedure gave us reasonable estimates.

Also in our present article our procedure is, in essence, to take the couplings of the particles as given by the MCPM in the strict symmetry limit but put in the correct masses of the first and second family fermions by hand. Our estimates, obtained in this way, should no be taken as precision predictions for experimental observables. Our intention here is to see what our MCPM estimates can say concerning the $\gamma\gamma$ events reported in [21].

We shall then discuss the leptonic decays of the charm-strange mesons D_s^\pm in the MCPM. We also give theoretical estimates for observables where the MCPM Higgs bosons should show up.

As already mentioned in the introduction we have in the MCPM after EWSB five physical Higgs bosons, three neutral ones ρ' , h' , h'' , and the charged pair H^\pm . With

$$v_0 = \sqrt{\frac{-\xi_0}{\eta_{00} + \mu_3}} = 246 \text{ GeV} \quad (20)$$

the standard Higgs-field vacuum-expectation value we find for the Higgs masses

$$\begin{aligned} m_{\rho'}^2 &= 2(-\xi_0) = 2v_0^2(\eta_{00} + \mu_3), \\ m_{h'}^2 &= 2v_0^2(\mu_1 - \mu_3), \\ m_{h''}^2 &= 2v_0^2(\mu_2 - \mu_3), \\ m_{H^\pm}^2 &= 2v_0^2(-\mu_3). \end{aligned} \quad (21)$$

A strict prediction of the MCPM is the following mass relation between the pseudoscalar h'' and the scalar h' ,

$$m_{h''} \leq m_{h'}. \quad (22)$$

The Feynman rules for these bosons are given explicitly in appendix A of [19]. The main feature of interest to us here is that h' and h'' have a scalar, respectively, pseudoscalar coupling to charm quarks with coupling constants proportional to the t quark mass divided by v_0 ; see Fig. 3. Both, h' and h'' , have the largest coupling to the charm quark. Numerically we have

$$c'_c = c''_c = \frac{m_t}{v_0} = \frac{173 \text{ GeV}}{246 \text{ GeV}} = 0.703. \quad (23)$$

This is of the order of an electromagnetic coupling

$$e = \sqrt{4\pi\alpha_{\text{em}}} = 0.303. \quad (24)$$

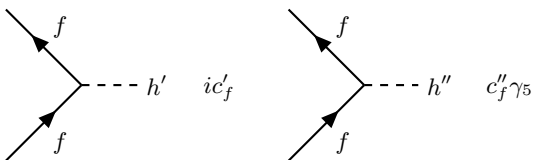


Figure 3. Couplings of the second-family fermions $f = \mu, c, s$ to the bosons h' and h'' . We have $c'_\mu = m_\tau/v_0$, $c'_c = m_t/v_0$, $c'_s = m_b/v_0$ and $c''_\mu = -m_\tau/v_0$, $c''_c = m_t/v_0$, $c''_s = -m_b/v_0$. Here $v_0 = 246 \text{ GeV}$ is the standard Higgs vacuum-expectation value.

Of course, parity is not conserved in the MCPM and the naming of h' (h'') scalar (pseudoscalar) is only a reminder of their scalar (pseudoscalar) coupling to fermions; see Fig. 3.

For the discussion of the leptonic decays of the mesons D_s^\pm in the MCPM we also need the couplings of H^\pm to fermions which we give in Fig. 4; see appendix A of [19]. In our model H^\pm only couple, concerning the fermions, to the $\mu\nu_\mu$ and cs combinations.

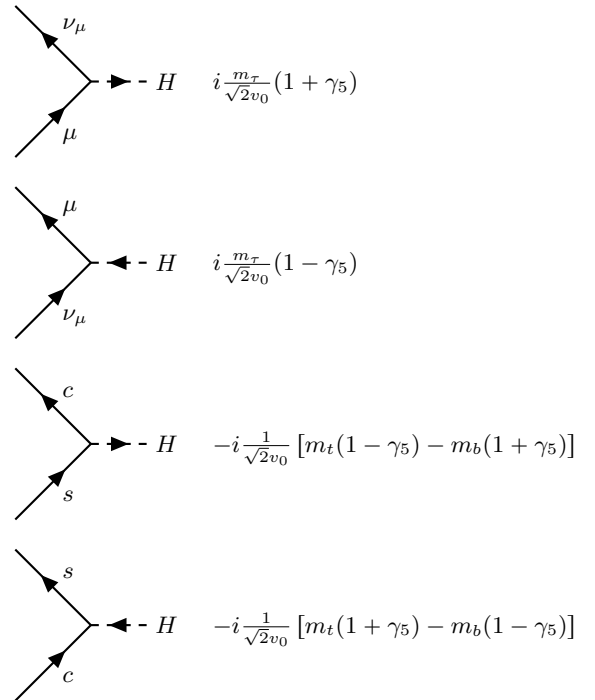


Figure 4. Couplings of H^\pm to fermions in the MCPM. The arrows on the H lines indicate the flow direction of H^- .

III. RESULTS

Since a mass value of 95.4 GeV seems rather low for a new Higgs boson we shall investigate in this chapter the consequences of having in the framework of the MCPM the boson h'' at this mass. The boson h' must then have a higher or equal mass; see (22). According to Fig. 8 of [19] the main decay mode of h'' with a mass around 100 GeV is $h'' \rightarrow c\bar{c}$. All other decay modes have a branching fraction of less than 10^{-3} . Thus we have for the expected total width $\Gamma_{h''}$ of such a h'' , with an accuracy at the per mille level, $\Gamma_{h''} \approx \Gamma(h' \rightarrow c\bar{c})$ and, therefore, from Table 3 of [19], with $m_{h''}$ in units of GeV,

$$\begin{aligned} \Gamma_{h''} &= 12.08 \times \frac{m_{h''}}{200} \text{ GeV} \\ &= 5.76 \text{ GeV for } m_{h''} = 95.4 \text{ GeV}. \end{aligned} \quad (25)$$

Its $\gamma\gamma$ width has been calculated in Sec. 3.3, (3.9)–(3.17), of [19]. For 95.4 GeV we get for this width and the corresponding branching fraction

$$\Gamma(h'' \rightarrow \gamma\gamma) = 3.26 \text{ keV}, \quad \text{B}(h'' \rightarrow \gamma\gamma) = 5.66 \cdot 10^{-7}. \quad (26)$$

Now we investigate the production of h'' in pp collisions followed by the decay $h'' \rightarrow \gamma\gamma$, see Fig. 5,

$$\begin{aligned} p(p_1, s_1) + p(p_2, s_2) &\rightarrow h''(k) + X. \\ &\quad \hookrightarrow \gamma(k_1, \epsilon_1) + \gamma(k_2, \epsilon_2) \end{aligned} \quad (27)$$

Here p_1, p_2, k, k_1, k_2 are the momenta of the particles, ϵ_1, ϵ_2 are the polarisation vectors of the photons, and s_1, s_2 are the spin indices of the protons.

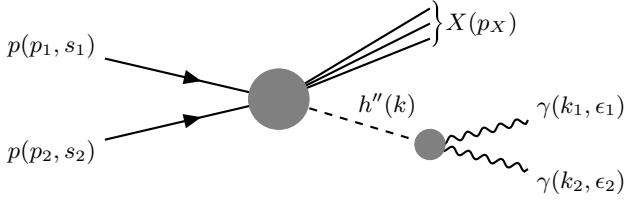


Figure 5. Diagram for the reaction (27), $p + p \rightarrow (h'' \rightarrow \gamma\gamma) + X$.

The amplitude for the reaction (27) is

$$i\langle\gamma(k_1, \epsilon_1), \gamma(k_2, \epsilon_2), X(p_X)|T|p(p_1, s_1), p(p_2, s_2)\rangle = i\langle\gamma(k_1, \epsilon_1), \gamma(k_2, \epsilon_2)|T|h''(k)\rangle \frac{i}{k^2 - m_{h''}^2 + im_{h''}\Gamma_{h''}} \times i\langle h''(k), X(p_X)|T|p(p_1, s_1), p(p_2, s_2)\rangle, \quad (28)$$

with $k = k_1 + k_2$. We are interested in the cross section with respect to the invariant $\gamma\gamma$ mass squared

$$m_{\gamma\gamma}^2 = (k_1 + k_2)^2. \quad (29)$$

We assume unpolarised initial protons, no observation of photon polarisations in the final state, and use $\Gamma_{h''} \ll m_{h''}$; see (25). Furthermore, we assume measurement of h'' , that is, the $\gamma\gamma$ system, in a certain phase-space region \mathcal{B} . We define the inclusive cross section for h'' production by

$$d\sigma_{\text{inc}}(p(p_1) + p(p_2) \rightarrow h''(k) + X) = \frac{d^3k}{k^0} f_{\text{inc}}(k) = \frac{d^3k}{k^0} \frac{1}{2\sqrt{s(s-4m_p^2)}} \frac{1}{2} \frac{1}{(2\pi)^3} \sum_X (2\pi)^4 \delta^{(4)}(k + p_X - p_1 - p_2) \times \frac{1}{4} \sum_{\text{spins}} |\langle h''(k), X(p_X)|T|p(p_1, s_1), p(p_2, s_2)\rangle|^2, \quad (30)$$

where $s = (p_1 + p_2)^2$ is the center-of-mass energy squared. The $\gamma\gamma$ width of h'' is given by

$$\Gamma(h'' \rightarrow \gamma\gamma) = \frac{1}{2m_{h''}} \frac{1}{2} \times \int \frac{d^3k_1}{(2\pi)^3 2k_1^0} \frac{d^3k_2}{(2\pi)^3 2k_2^0} (2\pi)^4 \delta^{(4)}(k_1 + k_2 - k) \times \sum_{\text{spins}} |\langle\gamma(k_1, \epsilon_1), \gamma(k_2, \epsilon_2)|T|h''(k)\rangle|^2, \quad (31)$$

where $k^2 = m_{h''}^2$. Putting everything together we get for $d\sigma/dm_{\gamma\gamma}^2$ with h'' in the phase-space region \mathcal{B}

$$\frac{d\sigma}{dm_{\gamma\gamma}^2}(p(p_1) + p(p_2) \rightarrow (h'' \rightarrow \gamma\gamma) + X)|_{\mathcal{B}} = \frac{\Gamma(h'' \rightarrow \gamma\gamma)}{\Gamma_{h''}} \frac{m_{h''}\Gamma_{h''}}{\pi} \times \frac{1}{(m_{\gamma\gamma}^2 - m_{h''}^2)^2 + m_{h''}^2\Gamma_{h''}^2} \int_{\mathcal{B}} \frac{d^3k}{k^0} f_{\text{inc}}(k). \quad (32)$$

Taking now \mathcal{B} to be the total phase space for h'' production and integrating over $m_{\gamma\gamma}^2$ we find finally

$$\sigma(p(p_1) + p(p_2) \rightarrow (h'' \rightarrow \gamma\gamma) + X) = \mathcal{B}(h'' \rightarrow \gamma\gamma) \times \sigma(p(p_1) + p(p_2) \rightarrow h'' + X). \quad (33)$$

In the MCPM the main direct production mode of the h'' is the Drell-Yan reaction with a charm plus an anticharm quark fusing to give h'' ; see Fig. 6. In addition

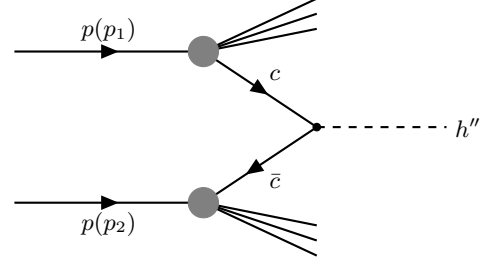


Figure 6. Drell-Yan process for production of h'' . The diagram with the roles of c and \bar{c} exchanged has to be added.

there is gluon-gluon fusion giving h'' (Fig. 7) and possibly also H^\pm production with the subsequent decays

$$H^\pm \rightarrow h'' + W^\pm; \quad (34)$$

see Fig. 8. The couplings $H^\pm h'' W$ are given in appendix A of [19]. Of course, the decays (34) can only occur if H^\pm are heavy enough,

$$m_{H^\pm} > m_{h''} + m_W = 175.8 \text{ GeV}. \quad (35)$$

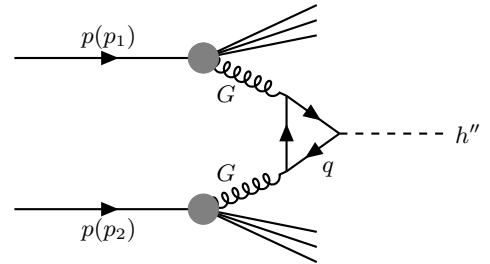


Figure 7. Production of h'' via gluon-gluon fusion with $q = c, s$.

We have adapted the calculations of [19] to our case here, $\sqrt{s} = 13 \text{ TeV}$ and $h'' = 95.4 \text{ GeV}$. We find the following cross sections

$$\sigma(p + p \rightarrow h'' + X) \Big|_{\text{DY}} = 13770.7 \text{ pb}, \quad (36)$$

$$\sigma(p + p \rightarrow h'' + X) \Big|_{\text{GG}} = 227.7 \text{ pb}. \quad (37)$$

The result for H^\pm production with subsequent decay (34) is shown in Fig. 9. Here also the value of the h' mass

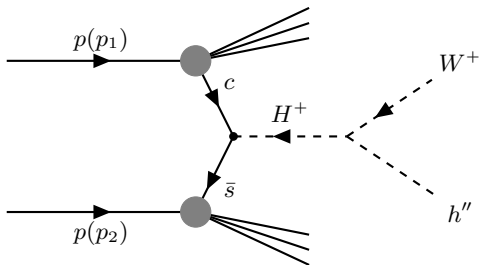


Figure 8. Drell-Yan production of H^+ with its subsequent decay to $W^+ + h''$. The diagram with the roles of c and \bar{s} exchanged has to be added. The diagrams for H^- production and decay to $W^- + h''$ are analogous.

enters through the calculation of the total width Γ_{H^\pm} and the branching fractions $B(H^\pm \rightarrow h'' + W^\pm)$. We show the results for the, in our framework here, lowest possible value for $m_{h'} = m_{h''} = 95.4$ GeV and for $m_{h'} = 1000$ GeV.

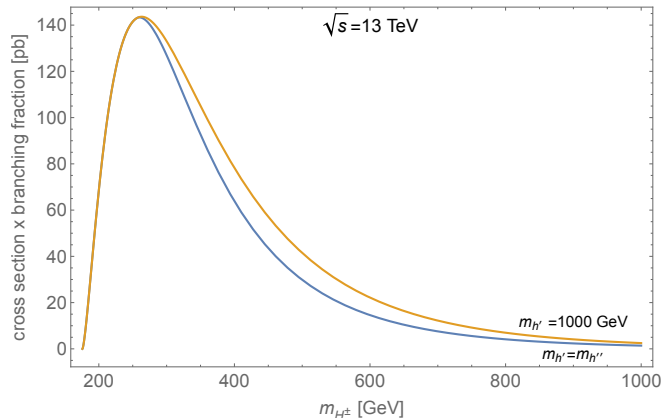


Figure 9. The result for $\sum_{l=\pm} \sigma(p + p \rightarrow H^l + X) \times B(H^l \rightarrow h'' + W^l)$ for $\sqrt{s} = 13$ TeV and $m_{h''} = 95.4$ GeV as function of the H^\pm mass m_{H^\pm} . In the lower curve the h' mass is set to $m_{h'} = m_{h''} = 95.4$ GeV and in the upper curve to $m_{h'} = 1000$ GeV.

In Fig. 10 we show the cross sections for the Drell-Yan reactions for production of h'' , h' , and H^\pm as functions of the Higgs-boson masses for $\sqrt{s} = 13$ TeV.

IV. COMPARISON WITH EXPERIMENT AND DISCUSSIONS

First we discuss $\sigma(p + p \rightarrow h'' + X) \times B(h'' \rightarrow \gamma + \gamma)$. From the CMS measurement we conclude that for 95.4 GeV there may be an enhancement of this type of product of the order of 0.01-0.04 pb; see (1) and Fig. 1. For our h'' with $m_{h''} = 95.4$ GeV we find on the other hand, using only the Drell-Yan (DY) and the gluon-gluon

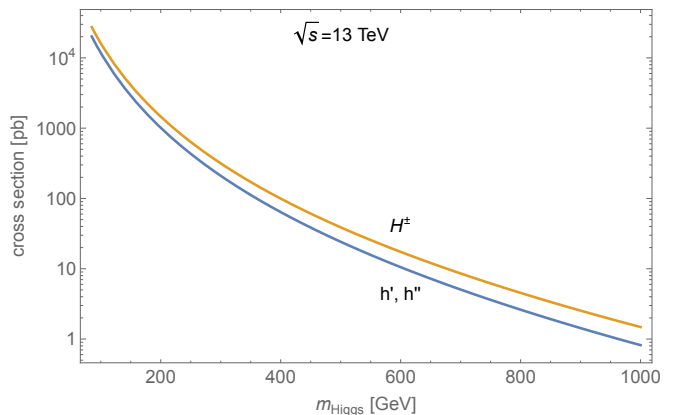


Figure 10. Cross sections for h'' , h' , and H^\pm production in pp collisions at $\sqrt{s} = 13$ TeV via the Drell-Yan reactions $c\bar{c} \rightarrow h''$, $c\bar{c} \rightarrow h'$, $c\bar{s} \rightarrow H^+$, and $s\bar{c} \rightarrow H^-$.

(GG) fusion contributions to $\sigma(p + p \rightarrow h'' + X)$,

$$\left[\sigma_{\text{DY}}(p + p \rightarrow h'' + X) + \sigma_{\text{GG}}(p + p \rightarrow h'' + X) \right] \times B(h'' \rightarrow \gamma + \gamma) = 0.0079 \text{ pb}; \quad (38)$$

see (26), (36), and (37). The product (38) is shown as function of the h'' mass in Fig. 11.

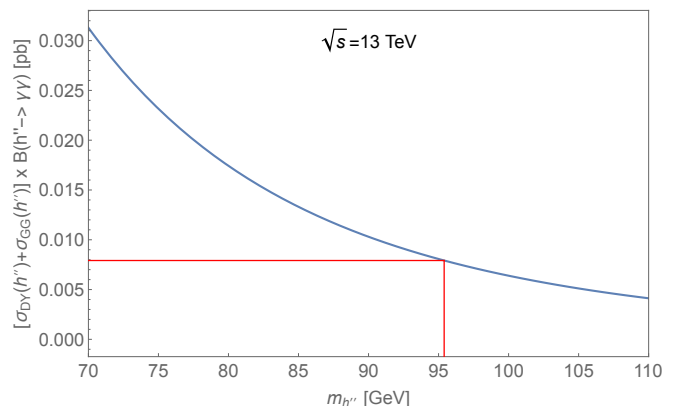


Figure 11. The product $[\sigma_{\text{DY}}(p + p \rightarrow h'' + X) + \sigma_{\text{GG}}(p + p \rightarrow h'' + X)] \times B(h'' \rightarrow \gamma + \gamma)$ for $\sqrt{s} = 13$ TeV as function of the h'' mass. The red lines correspond to $m_{h''} = 95.4$ GeV where the CMS experiment sees an enhancement; see Fig. 1.

It is remarkable that choosing in the MCPM the h'' mass $m_{h''} = 95.4$ GeV we find, without any tuning of other parameters, a value (38) which is within a factor of about two equal to the possible experimental result (1). Of course, this experimental *result* could be a statistical fluctuation. Then the above *agreement* with our theory would be completely fortuitous. But let us, in the following, tentatively assume that, indeed, the above experimental result indicates a new effect. We have then an experimental and some theoretical comments.

In [21] the analysis was done for a Standard-Model-like Higgs boson. We do not know if and how the results of [21] would change if this assumption is dropped and if the production modes for our boson h'' would be considered. It would be nice if the experimentalists could reanalyse their data in this way.

Our theoretical estimate for $\sigma_{\text{DY}}(p + p \rightarrow h'' + X)$ is almost certainly a lower limit for this cross section. We used only the leading-order Drell-Yan formula. For the usual Drell-Yan reactions, production of the vector bosons γ^* , Z , W^\pm , it is known that higher order corrections in α_s , the strong coupling parameter, increase σ_{DY} ; see for instance chapter 9.2 of [32]. We expect, therefore, also for our case a similar situation. Furthermore, for H^\pm with a mass $m_{H^\pm} > 175.8$ GeV, H^\pm production with subsequent decay $H^\pm \rightarrow h'' + W^\pm$ (34) will increase the h'' yield; see Fig. 9.

Encouraged by these considerations of a possible h'' boson at 95.4 GeV we are now looking at consequences for the Higgs bosons h' and H^\pm of the MCPM. For this we use the method of [33]. We consider the oblique parameters S , T , U which have been computed and compared to the electroweak precision data [28] giving

$$S = -0.02 \pm 0.10, \quad T = 0.03 \pm 0.12, \quad U = 0.01 \pm 0.11. \quad (39)$$

The masses of the Higgs bosons of the MCPM must respect the bounds on these parameters given in (39). Now we fix in the MCPM the masses of ρ' and h'' :

$$m_{\rho'} = 125.25 \text{ GeV}, \quad m_{h''} = 95.4 \text{ GeV}. \quad (40)$$

We get then 1σ , 2σ , and 3σ regions in the $m_{h'}-m_{H^\pm}$ plane as shown in Fig. 12. Interestingly we find an allowed 3σ interval for the mass of the charged Higgs bosons of the order of

$$45 \text{ GeV} < m_{H^\pm} < 300 \text{ GeV}. \quad (41)$$

The lower limit of $m_Z/2 \approx 45$ GeV comes from the fact that a decay $Z \rightarrow H^+ H^-$ has not been observed. The mass of h' is allowed to be up to 1000 GeV. But such high masses of h' are unreasonable in the model. To justify our perturbative treatment we should probably require the parameters of the potential (11), (12) to be not too large. But for $m_{h'} > 1000$ GeV we find from (21)

$$\mu_1 - \mu_3 = \frac{m_{h'}^2}{2v_0^2} > 8.2. \quad (42)$$

Thus, we consider $m_{h'} = 1000$ GeV as a generous upper limit up to which the MCPM still could make sense. For very high values of the quartic parameters μ_1 , μ_2 , μ_3 of the potential (11) we would have a strongly interacting Higgs sector where perturbative calculations would no longer be reliable.

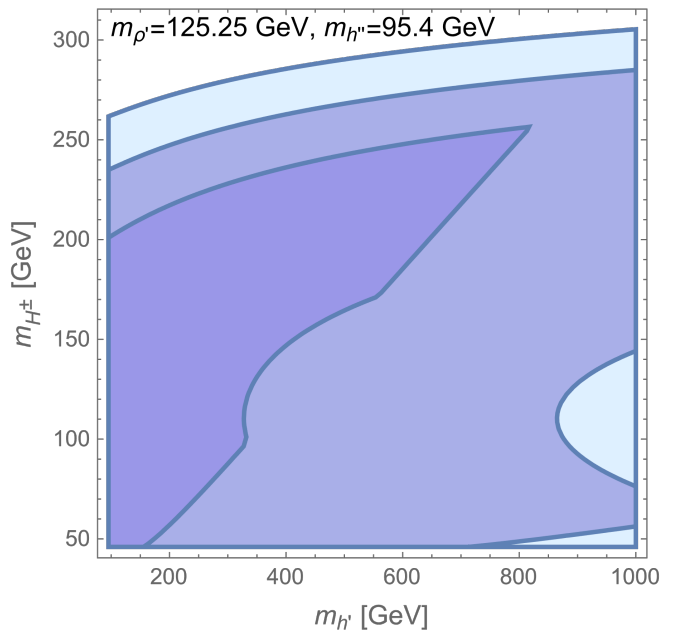


Figure 12. The allowed regions in the $m_{h'}-m_{H^\pm}$ plane due to the values of the S , T , U parameters (39). The masses of ρ' and h'' are fixed to $m_{\rho'} = 125.25$ GeV and $m_{h''} = 95.4$ GeV. The shaded areas correspond to the 1σ , 2σ , and 3σ uncertainties of S , T , U in (39).

V. LEPTONIC DECAYS OF D_s MESONS IN THE MCPM

In this section we shall discuss aspects of flavor physics in the MCPM, that is, physics governed by the CKM matrix V ; see (15). In the strict symmetry limit of the MCPM we have from (16) $V_{\text{MCPM}} = \mathbb{1}_3$. Thus we can only give estimates/predictions at present for reactions involving the diagonal elements of the CKM matrix. But let us note that in the SM there is no prediction or estimate for the CKM matrix which could in principle be any unitary matrix. In contrast to this, we have in the MCPM in the strict symmetry limit the result $V = \mathbb{1}_3$ which is quite a good approximation to what is found by experiments; see (18).

Keeping all this in mind we shall here study the leptonic decays of the charm-strange mesons D_s^\pm ,

$$D_s^+(p) \rightarrow l^+(k_1, s_1) + \nu_l(k_2, s_2), \quad (43)$$

$$D_s^-(p) \rightarrow l^-(k_1, s_1) + \bar{\nu}_l(k_2, s_2), \quad l = e, \mu, \tau. \quad (44)$$

Here p , k_1 , k_2 are the momenta and s_1 , s_2 the helicities of the particles. In the SM these decays proceed through W -boson exchange. In the MCPM we have in addition, for the muonic decay only, exchange of the H^\pm bosons; see Fig. 13

The decays (43) and (44) have been studied thoroughly in the literature; see e.g. [34, 35] and the review 72 of [28]. To leading order these low-energy processes are governed

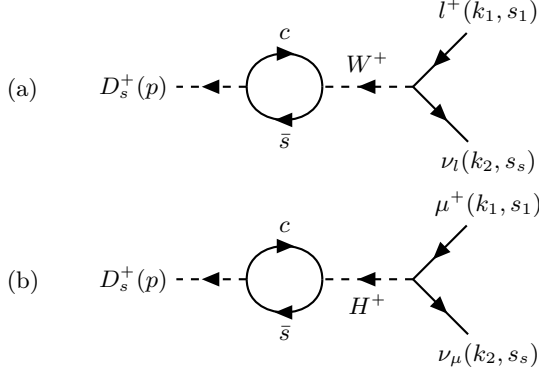


Figure 13. Diagrams of leading order for the leptonic decay of D_s^\pm . In (a) we have the W -exchange diagram for $l = e, \mu, \tau$, in (b) the H^\pm exchange diagram of the MCPM which contributes only to the muonic decay. The diagrams for D_s^- decay are analogous.

by effective Lagrangians. The exchange of the W gives

$$\mathcal{L}_{\text{eff}}^{(W)}(x) = -\frac{G_F}{\sqrt{2}} \sum_{l=e,\mu,\tau} \left\{ \begin{aligned} & \bar{\nu}_l(x) \gamma^\lambda (1 - \gamma_5) l(x) \bar{s}(x) V_{cs}^* \gamma_\lambda (1 - \gamma_5) c(x) \\ & + \bar{l}(x) \gamma^\lambda (1 - \gamma_5) \nu_l(x) \bar{c}(x) V_{cs} \gamma_\lambda (1 - \gamma_5) s(x) \end{aligned} \right\}, \quad (45)$$

where G_F is Fermi's constant and V_{cs} is the appropriate element of the Cabibbo-Kobayashi-Maskawa (CKM) matrix. The effective Lagrangian for H^\pm exchange reads, using the couplings shown in Fig. 4

$$\mathcal{L}_{\text{eff}}^{(H)}(x) = \frac{1}{m_{H^\pm}^2} J(x) J^\dagger(x). \quad (46)$$

Here we have with v_0 from (20)

$$\begin{aligned} J(x) &= \frac{m_\tau}{\sqrt{2}v_0} \bar{\mu}(x) (1 - \gamma_5) \nu_\mu(x) \\ &\quad - \frac{m_t - m_b}{\sqrt{2}v_0} \bar{s}(x) c(x) - \frac{m_t + m_b}{\sqrt{2}v_0} \bar{s}(x) \gamma_5 c(x), \\ J^\dagger(x) &= \frac{m_\tau}{\sqrt{2}v_0} \bar{\nu}_\mu(x) (1 + \gamma_5) \mu(x) \\ &\quad - \frac{m_t - m_b}{\sqrt{2}v_0} \bar{c}(x) s(x) + \frac{m_t + m_b}{\sqrt{2}v_0} \bar{c}(x) \gamma_5 s(x). \end{aligned} \quad (47)$$

In the following we shall calculate the matrix elements for the decays (43) and (44) in leading order neglecting neutrino masses and mixings. The hadronic parts of these matrix elements are then QCD quantities which have to respect parity (P), time-reversal (T) and charge-conjugation (C) invariance. We have

$$\begin{aligned} \langle 0 | \bar{c}(x) \gamma^\lambda \gamma_5 s(x) | D_s^-(p) \rangle &= \langle 0 | \bar{s}(x) \gamma^\lambda \gamma_5 c(x) | D_s^+(p) \rangle \\ &= ip^\lambda f_{D_s} e^{-ip \cdot x}, \quad f_{D_s}^* = f_{D_s}, \end{aligned} \quad (48)$$

and

$$\begin{aligned} \langle 0 | \bar{c}(x) \gamma_5 s(x) | D_s^-(p) \rangle &= \langle 0 | \bar{s}(x) \gamma_5 c(x) | D_s^+(p) \rangle \\ &= -im_{D_s} \tilde{f}_{D_s} e^{-ip \cdot x}, \quad \tilde{f}_{D_s}^* = \tilde{f}_{D_s}. \end{aligned} \quad (49)$$

For the following it is convenient to define

$$r = \left(\frac{f_{D_s}}{\tilde{f}_{D_s}} \right)^{1/2}. \quad (50)$$

The decay constant f_{D_s} has been computed by lattice QCD methods. A recent review [35] gives

$$f_{D_s} = (249.9 \pm 0.5) \text{ MeV}; \quad (51)$$

see also Table 72.4 of [28]. To estimate \tilde{f}_{D_s} we can use the divergence relation (see [34])

$$i \frac{\partial}{\partial x^\lambda} \bar{c}(x) \gamma^\lambda \gamma_5 s(x) = -(m_c + m_s) \bar{c}(x) \gamma_5 s(x). \quad (52)$$

This gives from (48) and (49)

$$\tilde{f}_{D_s} = \frac{m_{D_s}}{m_c + m_s} f_{D_s}. \quad (53)$$

The problem with (53) is that we do not know at which scale we should take the quark masses m_c and m_s . Using the $\overline{\text{MS}}$ masses as quoted in PDG [28] we get for f_{D_s}/\tilde{f}_{D_s} and $r = (f_{D_s}/\tilde{f}_{D_s})^{1/2}$

$$\frac{f_{D_s}}{\tilde{f}_{D_s}} = \frac{m_c + m_s}{m_{D_s}} = 0.69, \quad r = \sqrt{\frac{f_{D_s}}{\tilde{f}_{D_s}}} = 0.83. \quad (54)$$

But maybe we should, for the low energy decays (43) and (44), rather use constituent quark masses m_c and m_s . Therefore, we give now another estimate for \tilde{f}_{D_s} . We split the Dirac-field operators into upper and lower components,

$$c(x) = \begin{pmatrix} \varphi_c(x) \\ \chi_c(x) \end{pmatrix}, \quad s(x) = \begin{pmatrix} \varphi_s(x) \\ \chi_s(x) \end{pmatrix}. \quad (55)$$

We have then

$$\begin{aligned} \bar{c}(x) \gamma^0 \gamma_5 s(x) &= \varphi_c^\dagger(x) \chi_s(x) + \chi_c^\dagger(x) \varphi_s(x), \\ \bar{c}(x) \gamma_5 s(x) &= \varphi_c^\dagger(x) \chi_s(x) - \chi_c^\dagger(x) \varphi_s(x). \end{aligned} \quad (56)$$

For non-relativistic antiquark \bar{c} and quark s in the D_s^- state at rest, $p = p_R = (m_{D_s}, 0, 0, 0)^T$, we expect that only the terms $\chi_c^\dagger \varphi_s$ in (56) will contribute to $\langle 0 | \bar{c}(x) \gamma^0 \gamma_5 s(x) | D_s^-(p_R) \rangle$ and $\langle 0 | \bar{c}(x) \gamma_5 s(x) | D_s^-(p_R) \rangle$. Thus, we expect to have

$$\begin{aligned} \langle 0 | \bar{c}(x) \gamma^0 \gamma_5 s(x) | D_s^-(p_R) \rangle &\approx \langle 0 | \chi_c^\dagger(x) \varphi_s(x) | D_s^-(p_R) \rangle \\ &\approx -\langle 0 | \bar{c}(x) \gamma_5 s(x) | D_s^-(p_R) \rangle. \end{aligned} \quad (57)$$

From (48) and (49) we get then

$$\tilde{f}_{D_s} \approx f_{D_s}, \quad \frac{f_{D_s}}{\tilde{f}_{D_s}} \approx 1, \quad r = \sqrt{\frac{f_{D_s}}{\tilde{f}_{D_s}}} \approx 1. \quad (58)$$

In the following we shall, for our estimates, assume the ratio r (50) to be in the range

$$0.8 \leq r \leq 1.2. \quad (59)$$

Now we can calculate the T -matrix element for the decay (43) where we take the final state as

$$|l^+(k_1, s_1), \nu_l(k_2, s_2)\rangle = b_l^\dagger(k_1, s_1) a_{\nu_l}^\dagger(k_2, s_2) |0\rangle. \quad (60)$$

Here b^\dagger and a^\dagger are the appropriate creation operators. By (60) we have fixed the phase of the final state. In the SM we have only the W -exchange diagram, Fig. 13 (a), and we get the well known result

$$\begin{aligned} & \langle l^+(k_1, s_1), \nu_l(k_2, s_2) | T | D_s^+(p) \rangle_{\text{SM}} \\ &= i \frac{G_F}{\sqrt{2}} V_{cs}^* m_l f_{D_s} \bar{u}_{\nu_l}(k_2, s_2) (1 + \gamma_5) v_l(k_1, s_1), \quad l = e, \mu, \tau. \end{aligned} \quad (61)$$

For the decay rates this gives

$$\begin{aligned} & \Gamma(D_s^+ \rightarrow l^+ \nu_l)_{\text{SM}} \\ &= \frac{G_F^2}{8\pi} |f_{D_s}|^2 |V_{cs}|^2 m_{D_s} m_l^2 \left(1 - \frac{m_l^2}{m_{D_s}^2}\right)^2, \quad l = e, \mu, \tau. \end{aligned} \quad (62)$$

The factors m_l in (61) and m_l^2 in (62) are the famous helicity-suppression factors which lead to the hierarchy

$$\begin{aligned} & \Gamma(D_s^+ \rightarrow e^+ \nu_e)_{\text{SM}} \\ & \ll \Gamma(D_s^+ \rightarrow \mu^+ \nu_\mu)_{\text{SM}} \\ & \ll \Gamma(D_s^+ \rightarrow \tau^+ \nu_\tau)_{\text{SM}}. \end{aligned} \quad (63)$$

We note that the SM decay rates (62) contain the factor $|V_{cs}|^2$ which, a priori, is not fixed in the SM, except for $0 \leq |V_{cs}|^2 \leq 1$. Thus, these decay rates are one possibility to *determine* $|V_{cs}|$, and this is indeed what is done. Taking our leading order calculation (62) for the $\tau^+ \nu_\tau$ decay we get with the masses and the total width Γ_{D_s} from PDG [28],

$$\begin{aligned} & B(D_s^+ \rightarrow \tau^+ \nu_\tau)_{\text{SM}} \\ &= |V_{cs}|^2 \frac{G_F^2}{8\pi} |f_{D_s}|^2 m_{D_s} m_\tau^2 \left(1 - \frac{m_\tau^2}{m_{D_s}^2}\right)^2 \Gamma_{D_s}^{-1} \\ &= |V_{cs}|^2 \cdot 5.51 \times 10^{-2}. \end{aligned} \quad (64)$$

Comparing this with the experimental value from PDG [28],

$$B(D_s^+ \rightarrow \tau^+ \nu_\tau)_{\text{exp}} = (5.32 \pm 0.11) \times 10^{-2} \quad (65)$$

we get, taking the central value from (65),

$$|V_{cs}| = 0.982. \quad (66)$$

This is close to the value $|V_{cs}| = 0.975 \pm 0.006$ which is obtained taking into account experimental results for leptonic plus semileptonic D_s decays and theoretical corrections in the SM calculations; see (12.10) of the review 12 of [28].

Finally we consider the ratio

$$R_{\tau\mu} = \frac{\Gamma(D_s^+ \rightarrow \tau^+ \nu_\tau)}{\Gamma(D_s^+ \rightarrow \mu^+ \nu_\mu)}. \quad (67)$$

In the SM this ratio is fixed, as there $|V_{cs}|^2$ drops out:

$$R_{\tau\mu}|_{\text{SM}} = \frac{m_\tau^2 \left(1 - \frac{m_\tau^2}{m_{D_s}^2}\right)^2}{m_\mu^2 \left(1 - \frac{m_\mu^2}{m_{D_s}^2}\right)^2}. \quad (68)$$

With the masses of the particles from PDG [28] we get

$$R_{\tau\mu}|_{\text{SM}} = 9.75; \quad (69)$$

see (72.27) of [28]. There, the experimental value is quoted as

$$R_{\tau\mu}|_{\text{exp}} = 9.82 \pm 0.40. \quad (70)$$

Now we come to the decays (43) and (44) in the MCPM, remembering that our predictions should be considered as reasonable *estimates* as discussed in Sec. II. In the MCPM we have for the decay $D_s^+ \rightarrow l^+ \nu_l$ with $l = e, \tau$ the prediction as in (62) but setting $V_{cs} = 1$. Thus, we predict in the MCPM

$$\Gamma(D_s^+ \rightarrow \tau^+ \nu_\tau)_{\text{MCPM}} = \frac{G_F^2}{8\pi} |f_{D_s}|^2 m_{D_s} m_\tau^2 \left(1 - \frac{m_\tau^2}{m_{D_s}^2}\right)^2, \quad (71)$$

$$B(D_s^+ \rightarrow \tau^+ \nu_\tau)_{\text{MCPM}} = 5.51 \times 10^{-2}. \quad (72)$$

This agrees with experiment (65) to within 3.6% or 1.7 σ .

For the decay $D_s^+ \rightarrow \mu^+ \nu_\mu$ we have in the MCPM both, the W - and the H -exchange diagram; see Fig. 13. This gives

$$\begin{aligned} & \langle \mu^+(k_1, s_1), \nu_\mu(k_2, s_2) | T | D_s^+(p) \rangle_{\text{MCPM}} \\ &= i \frac{G_F}{\sqrt{2}} m_\mu f_{D_s} \left[1 - \frac{\bar{m}^2}{r^2 m_{H^\pm}^2} \right] \bar{u}_{\nu_\mu}(k_2, s_2) (1 + \gamma_5) v_\mu(k_1, s_1), \end{aligned} \quad (73)$$

where r is defined in (50) and

$$\bar{m}^2 = \frac{m_\tau(m_t + m_b)}{2v_0^2} \frac{\sqrt{2} m_{D_s}}{G_F m_\mu} = (76.5 \text{ GeV})^2. \quad (74)$$

From (71) and (73) we get for the ratio $R_{\tau\mu}$ (67) in the MCPM

$$R_{\tau\mu}|_{\text{MCPM}} = \frac{m_\tau^2 \left(1 - \frac{m_\tau^2}{m_{D_s}^2}\right)^2}{m_\mu^2 \left(1 - \frac{m_\mu^2}{m_{D_s}^2}\right)^2} \left(1 - \frac{\bar{m}^2}{r^2 m_{H^\pm}^2}\right)^{-2}. \quad (75)$$

Note that in the SM $\Gamma(D_s^+ \rightarrow \tau^+ \nu_\mu)$ contains the free parameter $|V_{cs}|$ and $R_{\tau\mu}$ is fixed; see (62) and (68), respectively. In the strict symmetry limit of the MCPM the situation is reversed: $\Gamma(D_s^+ \rightarrow \tau^+ \nu_\mu)$ is fixed, and $R_{\tau\mu}$ contains the free parameter m_{H^\pm} ; see (71) and (75), respectively.

In Fig. 14 we show $R_{\tau\mu}|_{\text{MCPM}}$ as function of rm_{H^\pm} and the experimental value $R_{\tau\mu}|_{\text{exp}}$ from (70). We find agreement of the MCPM prediction with the experimental value at the 1σ , 2σ , and 3σ level for

$$\begin{aligned} r \cdot m_{H^\pm} &\geq 500 \text{ GeV} && \text{at } 1\sigma \text{ level.} \\ r \cdot m_{H^\pm} &\geq 373 \text{ GeV} && \text{at } 2\sigma \text{ level.} \\ r \cdot m_{H^\pm} &\geq 313 \text{ GeV} && \text{at } 3\sigma \text{ level.} \end{aligned} \quad (76)$$

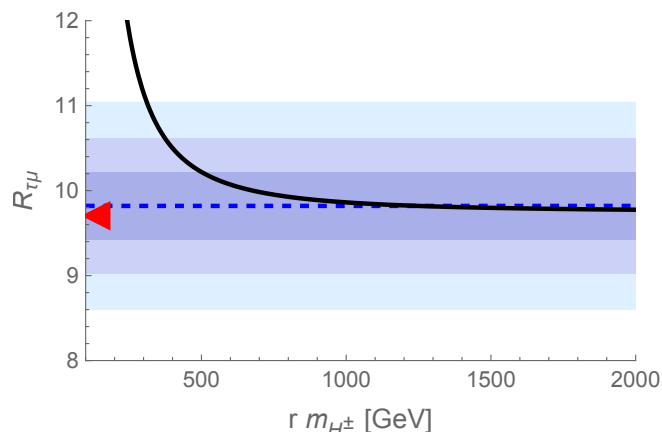


Figure 14. The ratio $R_{\tau\mu}$ (67). Shown are the experimental value with its one, two, and three sigma deviations as shaded regions, and the prediction of the MCPM (75) as function of rm_{H^\pm} (full line). A small triangle at the ordinate shows the prediction of the SM.

With the ratio r in the range (59) this translates to

$$\begin{aligned} m_{H^\pm} &\geq 416 \text{ GeV} && \text{at } 1\sigma \text{ level.} \\ m_{H^\pm} &\geq 311 \text{ GeV} && \text{at } 2\sigma \text{ level.} \\ m_{H^\pm} &\geq 261 \text{ GeV} && \text{at } 3\sigma \text{ level.} \end{aligned} \quad (77)$$

VI. CONCLUSIONS

In this work we have explored the consequences of assuming that the possible *anomaly* seen by CMS [21] in the $\gamma\gamma$ yield at 95.4 GeV may be due to production and decay of the h'' boson of the MCPM.

We found from our calculation for the product $\sigma(p + p \rightarrow h'' + X) \times \text{B}(h'' \rightarrow \gamma + \gamma) \approx 0.01 \text{ pb}$. We argued that this should be considered rather as a lower limit from theory. How could experimentalists explore the consequences of this finding further?

The MCPM gives also predictions for the decay $h'' \rightarrow \mu^+ \mu^-$ from the coupling shown in Fig. 3,

$$\begin{aligned} \Gamma(h'' \rightarrow \mu^+ \mu^-) &= 0.198 \text{ MeV}, \\ \text{B}(h'' \rightarrow \mu^+ \mu^-) &= 3.44 \times 10^{-5}. \end{aligned} \quad (78)$$

Therefore, we have the prediction for $m_{h''} = 95.4 \text{ GeV}$

$$\begin{aligned} [\sigma_{\text{DY}}(p + p \rightarrow h'' + X) + \sigma_{\text{GG}}(p + p \rightarrow h'' + X)] \\ \times \text{B}(h'' \rightarrow \mu^+ + \mu^-) = 0.481 \text{ pb}. \end{aligned} \quad (79)$$

But $m_{h''} = 95.4 \text{ GeV}$ is rather close to the Z mass $m_Z \approx 91.2 \text{ GeV}$ and the decay $Z \rightarrow \mu^+ \mu^-$ will present a large source of background. Maybe one could consider the ratio of $\mu^+ \mu^-$ and $e^+ e^-$ production. For $\mu^+ \mu^-$ the boson h'' will contribute but *not* for $e^+ e^-$.

Finally, the best way to establish the h'' would be to observe its main decay $h'' \rightarrow c\bar{c}$, that is, $h'' \rightarrow$ charm jet plus anticharm jet. Clearly, this represents a formidable challenge from the experimental side given the background from QCD $c\bar{c}$ jets and $Z \rightarrow c\bar{c}$ decays. The possibility to observe the production of h'' with subsequent decay to charm jets plus anticharm jet will depend on how well charm tagging can be done and what a resolution of the invariant mass of two such tagged jets can be achieved. Such an experimental study is far beyond the scope of this article, where we focus on the theoretical predictions. In this context it may be very advantageous to consider diffractive production of the h'' in pp collisions, where the h'' is produced in pomeron-pomeron (\mathbb{P} - \mathbb{P}) collisions. This type of reactions was first discussed in [36], where two processes were identified, the inclusive and exclusive one; see Figs. 1 and 2 of [36]. In the exclusive case we have $\mathbb{P} + \mathbb{P} \rightarrow h''$, that is,

$$p + p \rightarrow p + h'' + p. \quad (80)$$

In the inclusive case we have $\mathbb{P} + \mathbb{P} \rightarrow h'' + X$, where X would consist of two (presumably rather low energy) gluonic jets close to beam direction

$$p + p \rightarrow p + h'' + X + p. \quad (81)$$

In [36] numerical estimates for Higgs production via the inclusive reaction (81) were presented. Numerical results for the exclusive Higgs-production reaction (80) were first presented in [37]. For reviews of exclusive SM-Higgs production we refer to [38–41].

Studying the reactions (80) and (81) will require measurement of the outgoing protons, that is, it would need forward detectors. Then one could make a missing-mass analysis for detecting the possible production of h'' and with a central detector the remnant X in (81)

and the decays of h'' could be analysed. Presumably, in such a setup there will be much less background than in normal inclusive h'' production, where it will be accompanied by a large number of SM particles. The exclusive process (80) also offers the possibility to check the pseudoscalar couplings to fermions of the boson h'' . For this one could use the methods explained in [42, 43].

In Sec. V we have discussed MCPM effects in the leptonic decays of the charm-strange mesons D_s^\pm . The MCPM gave us a prediction/estimate for the decay rate of $D_s^+ \rightarrow \tau^+ \nu_\tau$ without free parameters. The corresponding branching fraction agrees with experiment at the level of 3.6% corresponding to 1.7σ .

Then we studied the ratio $R_{\tau\mu}$ of the decay rates to $\tau\nu_\tau$ and $\mu\nu_\mu$ leptons; see Fig. 14. From this we concluded that the charged Higgs-bosons H^\pm of the MCPM should have a mass $m_{H^\pm} \gtrsim 261$ GeV. On the other hand, our study of the oblique parameters S, T, U in Fig. 12 suggested $m_{H^\pm} \lesssim 300$ GeV. Thus, we have in the MCPM the prediction that there should be a pair of charged Higgs bosons H^\pm at a mass around $m_{H^\pm} \approx 300$ GeV. The main production mode of H^\pm at the LHC should be the Drell-Yan reaction with $c\bar{s}$ and $s\bar{c}$ fusion, see Fig. 8, where also the subsequent decay $H^+ \rightarrow W^+ h''$ is indicated. The Drell-Yan production cross sections for the H^\pm bosons are shown in Fig. 10.

In Fig. 15 we show the branching fractions of H^\pm as calculated in the MCPM. This is an update of Fig. 9 of [19]. In our present figure we have set the mass of the scalar boson h' to $m_{h'} = 200$ GeV. A higher mass $m_{h'}$ would shift the threshold of the decay channel $H^+ \rightarrow h' + W^+$ to the right, that is, to higher values of m_{H^+} . The main decay mode of a H^\pm with a mass around $m_{H^\pm} = 300$ GeV is predicted to be $H^+ \rightarrow c\bar{s}$, that is, the decay to a charm plus a strange jet. But a notable decay mode with a branching fraction around 21% is predicted to be $H^+ \rightarrow h'' + W^+$. This could give an interesting signal for experimental searches, since the W^+ should rather easily be detectable through its decays.

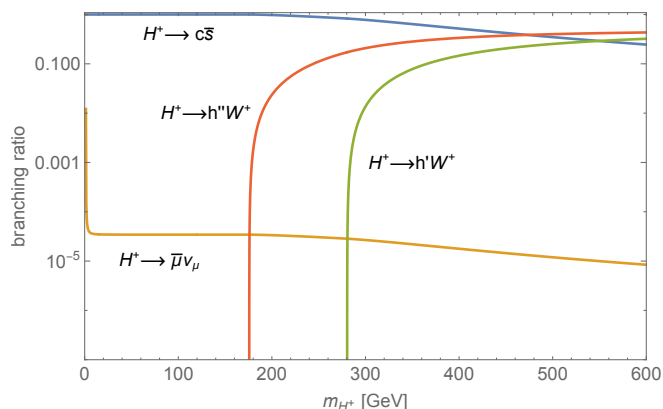


Figure 15. Branching fractions for the H^+ Higgs-boson decay channels as functions of m_{H^+} . We have set $m_{h''} = 95.4$ GeV and $m_{h'} = 200$ GeV.

Finally we can ask about effects of the MCPM in other areas of particle physics, for instance, involving top and bottom quarks and τ leptons. As stated in [17] and recalled here in Sec. II these fermions have in the MCPM exactly the same couplings to the MCPM boson ρ' as they have in the SM to the SM Higgs boson. Also, ρ' behaves very much like the SM Higgs boson; see the list of Feynman rules of the MCPM in [19]. Thus, MCPM effects involving $t, b,$ and τ fermions distinct from SM effects are expected to be very small. Next we can ask about MCPM effects for particles containing charm quarks. Exchange of the h'' will contribute to the $c\bar{c}$ potential; see Fig. 16. But due to (23) this will be a weak correction

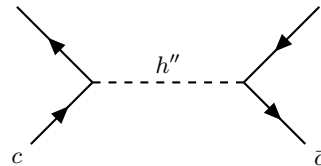


Figure 16. Diagram for h'' exchange contributing to the $c\bar{c}$ potential.

to the strong $c\bar{c}$ potential, similar to Z exchange. Thus, it will be hard to observe this h'' effect. In decays like

$$J/\Psi \rightarrow \text{hadrons} + (h'' \rightarrow \mu^+ \mu^-) \quad (82)$$

the virtual h'' has a coupling of the order of the electromagnetic one to the charm quarks; see (23), (24). But its couplings to $\mu^+ \mu^-$ is (see Fig. 3)

$$c_\mu'' = -\frac{m_\tau}{v_0} = -\frac{1.777 \text{ GeV}}{246 \text{ GeV}} = -7.2 \cdot 10^{-3}. \quad (83)$$

Thus, $|c_\mu''|$ is much smaller than e (24), and decays like (82) are expected to be extremely rare, much rarer than weak decays of the J/Ψ !

To conclude: motivated by the findings of CMS [21] we have explored the consequences of having the pseudoscalar Higgs boson h'' of the MCPM at a mass of 95.4 GeV. We have presented arguments from a study of the oblique parameters and of D_s leptonic decays that the charged Higgs-boson pair H^\pm of the MCPM should have a mass m_{H^\pm} around 300 GeV. We have then given a number of predictions which experimentalists working at LHC should be able to check. Thus, as it should be, our theory is falsifiable.

ACKNOWLEDGMENTS

We thank Christian Schwanenberger for very useful discussions and information concerning the CMS experimental results. We also thank A. Szczurek for discussions and comments. This work is supported by Chile ANID FONDECYT project 1200641.

- [1] ATLAS collaboration, *A detailed map of Higgs boson interactions by the ATLAS experiment ten years after the discovery*, *Nature* **607** (2022) 52 [2207.00092].
- [2] T.D. Lee, *A Theory of Spontaneous T Violation*, *Phys. Rev. D* **8** (1973) 1226.
- [3] W. Bernreuther, T. Schröder and T.N. Pham, *CP violating dipole form-factors in $e^+e^- \rightarrow \bar{t}t$* , *Phys. Lett. B* **279** (1992) 389.
- [4] A. Arhrib and G. Moulhaka, *Radiative corrections to $e^+e^- \rightarrow H^+H^-$: THDM versus MSSM*, *Nucl. Phys. B* **558** (1999) 3 [hep-ph/9808317].
- [5] J.F. Gunion, H.E. Haber, G.L. Kane and S. Dawson, *The Higgs Hunter's Guide*, vol. 80, Front. Phys. (2000).
- [6] M. Krawczyk, *Precision muon $g-2$ results and light Higgs bosons in the 2HDM(II)*, *Acta Phys. Polon. B* **33** (2002) 2621 [hep-ph/0208076].
- [7] P.M. Ferreira, M. Maniatis, O. Nachtmann and J.P. Silva, *CP properties of symmetry-constrained two-Higgs-doublet models*, *JHEP* **08** (2010) 125 [1004.3207].
- [8] G.C. Branco, P.M. Ferreira, L. Lavoura, M.N. Rebelo, M. Sher and J.P. Silva, *Theory and phenomenology of two-Higgs-doublet models*, *Phys. Rept.* **516** (2012) 1 [1106.0034].
- [9] L. Basso, A. Lipniacka, F. Mahmoudi, S. Moretti, P. Osland, G.M. Pruna et al., *Probing the charged Higgs boson at the LHC in the CP-violating type-II 2HDM*, *JHEP* **11** (2012) 011 [1205.6569].
- [10] M. Krause, M. Mühlleitner, R. Santos and H. Ziesche, *Higgs-to-Higgs boson decays in a 2HDM at next-to-leading order*, *Phys. Rev. D* **95** (2017) 075019 [1609.04185].
- [11] P. Basler, M. Mühlleitner and J. Wittbrodt, *The CP-Violating 2HDM in Light of a Strong First Order Electroweak Phase Transition and Implications for Higgs Pair Production*, *JHEP* **03** (2018) 061 [1711.04097].
- [12] M. Maniatis, L. Sartore and I. Schienbein, *Multiple point principle in the general Two-Higgs-Doublet model*, *JHEP* **08** (2020) 158 [2001.10541].
- [13] P.M. Ferreira, B. Grzadkowski, O.M. Ogreid and P. Osland, *Symmetries of the 2HDM: an invariant formulation and consequences*, *JHEP* **02** (2021) 196 [2010.13698].
- [14] L. Wang, J.M. Yang and Y. Zhang, *Two-Higgs-doublet models in light of current experiments: a brief review*, *Arxiv:2203.07244*.
- [15] J.L. Diaz-Cruz, R. Noriega-Papaqui and A. Rosado, *Mass matrix ansatz and lepton flavor violation in the THDM-III*, *Phys. Rev. D* **69** (2004) 095002 [hep-ph/0401194].
- [16] P.M. Ferreira, B. Grzadkowski, O.M. Ogreid and P. Osland, *New symmetries of the two-Higgs-doublet model*, *Eur. Phys. J. C* **84** (2024) 234 [2306.02410].
- [17] M. Maniatis, A. von Manteuffel and O. Nachtmann, *A New type of CP symmetry, family replication and fermion mass hierarchies*, *Eur. Phys. J. C* **57** (2008) 739 [0711.3760].
- [18] M. Maniatis, O. Nachtmann and A. von Manteuffel, *On the phenomenology of a two-Higgs-doublet model with maximal CP symmetry at the LHC: Synopsis and addendum*, in *Physics at the LHC 2010*, pp. 403–405, 9, 2010, DOI [1009.1869].
- [19] M. Maniatis and O. Nachtmann, *On the phenomenology of a two-Higgs-doublet model with maximal CP symmetry at the LHC*, *JHEP* **05** (2009) 028 [0901.4341].
- [20] M. Maniatis and O. Nachtmann, *On the phenomenology of a two-Higgs-doublet model with maximal CP symmetry at the LHC. II. Radiative effects*, *JHEP* **04** (2010) 027 [0912.2727].
- [21] CMS collaboration, *Search for a standard model-like Higgs boson in the mass range between 70 and 110 GeV in the diphoton final state in proton-proton collisions at $\sqrt{s} = 13$ TeV*, *CMS-PAS-HIG-20-002* (2023).
- [22] S. Bhattacharya, G. Coloretti, A. Crivellin, S.-E. Dahbi, Y. Fang, M. Kumar et al., *Growing Excesses of New Scalars at the Electroweak Scale*, 2306.17209.
- [23] T. Biekötter, S. Heinemeyer and G. Weiglein, *The CMS di-photon excess at 95 GeV in view of the LHC Run 2 results*, *Phys. Lett. B* **846** (2023) 138217 [2303.12018].
- [24] G. Coloretti, A. Crivellin and B. Mellado, *Combined Explanation of LHC Multi-Lepton, Di-Photon and Top-Quark Excesses*, 2312.17314.
- [25] F. Nagel, *New aspects of gauge-boson couplings and the Higgs sector*, Ph.D. thesis, University Heidelberg, 2004. <http://www.ub.uni-heidelberg.de/archiv/4803>.
- [26] M. Maniatis, A. von Manteuffel, O. Nachtmann and F. Nagel, *Stability and symmetry breaking in the general two-Higgs-doublet model*, *Eur. Phys. J. C* **48** (2006) 805 [hep-ph/0605184].
- [27] M. Maniatis, A. von Manteuffel and O. Nachtmann, *CP violation in the general two-Higgs-doublet model: A Geometric view*, *Eur. Phys. J. C* **57** (2008) 719 [0707.3344].
- [28] PARTICLE DATA GROUP collaboration, *Review of Particle Physics*, *PTEP* **2022** (2022) 083C01.
- [29] L. Wolfenstein, *Parametrization of the Kobayashi-Maskawa Matrix*, *Phys. Rev. Lett.* **51** (1983) 1945.
- [30] A.J. Buras, M.E. Lautenbacher and G. Ostermaier, *Waiting for the top quark mass, $K^+ \rightarrow \pi^+$ neutrino anti-neutrino, $B(s)0$ - anti- $B(s)0$ mixing and CP asymmetries in B decays*, *Phys. Rev. D* **50** (1994) 3433 [hep-ph/9403384].
- [31] CKMFITTER GROUP collaboration, *CP violation and the CKM matrix: Assessing the impact of the asymmetric B factories*, *Eur. Phys. J. C* **41** (2005) 1 [hep-ph/0406184].
- [32] R.K. Ellis, W.J. Stirling and B.R. Webber, *QCD and collider physics*, Cambridge University Press (1996), 10.1017/CBO9780511628788.
- [33] M. Maniatis and O. Nachtmann, *Symmetries and renormalisation in two-Higgs-doublet models*, *JHEP* **11** (2011) 151 [1106.1436].
- [34] B.A. Dobrescu and A.S. Kronfeld, *Accumulating evidence for nonstandard leptonic decays of D_s mesons*, *Phys. Rev. Lett.* **100** (2008) 241802 [0803.0512].
- [35] FLAVOUR LATTICE AVERAGING GROUP (FLAG) collaboration, *FLAG Review 2021*, *Eur. Phys. J. C* **82** (2022) 869 [2111.09849].
- [36] A. Schäfer, O. Nachtmann and R. Schöpf, *Production of Higgs particles in diffractive hadron-hadron collisions*,

- Phys. Lett. B* **249** (1990) 331.
- [37] A. Bialas and P.V. Landshoff, *Higgs production in $p p$ collisions by double pomeron exchange*, *Phys. Lett. B* **256** (1991) 540.
- [38] M.G. Albrow and A. Rostovtsev, *Searching for the Higgs at hadron colliders using the missing mass method*, [hep-ph/0009336](#).
- [39] J. Bartels, S. Bondarenko, K. Kutak and L. Motyka, *Exclusive Higgs boson production at the LHC: Hard rescattering corrections*, *Phys. Rev. D* **73** (2006) 093004 [[hep-ph/0601128](#)].
- [40] L.A. Harland-Lang, V.A. Khoze, M.G. Ryskin and W.J. Stirling, *Latest Results in Central Exclusive Production: A Summary*, in *7th International Workshop on Diffraction in High Energy Physics*, 1, 2013 [[1301.2552](#)].
- [41] LHC HIGGS CROSS SECTION WORKING GROUP collaboration, *Handbook of LHC Higgs Cross Sections: 3. Higgs Properties*, [1307.1347](#).
- [42] A.B. Kaidalov, V.A. Khoze, A.D. Martin and M.G. Ryskin, *Central exclusive diffractive production as a spin-parity analyser: From Hadrons to Higgs*, *Eur. Phys. J. C* **31** (2003) 387 [[hep-ph/0307064](#)].
- [43] P. Lebiedowicz, O. Nachtmann and A. Szczurek, *Exclusive central diffractive production of scalar and pseudoscalar mesons tensorial vs. vectorial pomeron*, *Annals Phys.* **344** (2014) 301 [[1309.3913](#)].